

Transient Flow of a Generalized Second Grade Fluid Due to a Constant Surface Shear Stress: an Approximate Integral-Balance Solution

Jordan Hristov

Abstract – Integral balance solution to start-up problem of a second grade viscoelastic fluid caused by a constant surface stress at the surface has been developed by an entire-domain parabolic profile with an unspecified exponent. The closed form solution explicitly defines two dimensionless similarity variables $\xi = y/\sqrt{vt}$ and $D_0 = \chi^2 = \sqrt{p/vt^\beta}$, responsible for the viscous and the elastic responses of the fluid to the step jump at the boundary. Numerical simulations demonstrating the effect of the various operating parameter and fluid properties on the developed flow field, as well comparison with the existing exact solutions have been performed. Numerical test with variable exponent of the approximate profile have been performed as a step improving the approximate solution. **Copyright** © 2011 Praise Worthy Prize S.r.l. - All rights reserved.

Keywords: Start-Up Problem, Surface Shear Stress, Viscoelastic, Integral-Balance Solution

I. Introduction

Transient flows of viscoelastic fluids are intensively modeled by analytical and numerical methods [1],[2],[3],[4],[5],[6] with very few exact analytical solutions obtained. The second grade fluid is the common non-Newtonian viscoelastic fluid in industrial fields, such as polymer solution [7], emulsions [8], crude oils [9], extrusion masses [10],[11], blood flow [12],[13] and magneto-hydrodynamic flows with heat and mass transfer [2]. Fractional calculus allows incorporating memory effects in the constitutive equations [14] by the fractional order time Riemann-Liouville derivative. The start-up flows of second grade generalized fluids have been intensively studied toward development of exact analytical solutions [4],[5],[15],[16] with Caputo derivatives, applying mainly Laplace transforms and consequent expressions by the generalized Mittag-Leffler function.

This article develops an approximate integral balance solution of a fractional generalized second fluid with a special emphasis on simplicity and physical adequacy, without significant loss of exactness and avoiding both the use of the Caputo derivative and the Laplace transforms.

II. Problem Statement

II.1. Constitutive Relationships

Generally, the constitutive relationship of the second grade fluids, that is thermodynamically compatible, is

defined as [17], [18]:

$$\mathbf{T} = -\rho\mathbf{I} + \mu \left[\text{grad}\mathbf{V} + (\text{grad}\mathbf{V})^T \right] + \left[D_t^\beta \left[\text{grad}\mathbf{V} + (\text{grad}\mathbf{V})^T \right] + \alpha_1 \left[\text{grad}\mathbf{V} + (\text{grad}\mathbf{V})^T \right] (\text{grad}\mathbf{V}) + \alpha_2 \left[\text{grad}\mathbf{V} + (\text{grad}\mathbf{V})^T \right]^2 \right] + \quad (1)$$

$$\mu \geq 0, \alpha_1 \geq 0, \alpha_1 + \alpha_2 = 0$$

In (1) ρ is the density, \mathbf{I} is the unit vector, while α_1 and α_2 are the normal stress moduli [17]. The coefficient $\alpha_1 \left[\rho y^2 / \mu \right]^\beta$ is the first normal stress modulus. The Riemann- Liouville operator D_t^β denotes:

$$D_t^\beta = \frac{1}{\Gamma(1-\beta)} \frac{d}{dt} \int_0^t \frac{f(\tau)}{(t-\tau)^\beta} d\tau, 0 < \beta < 1 \quad (2)$$

a model of a general second grade fluid .With $\beta = 0$ and $\alpha_1 = 0$ we get a classical Newtonian liquid, while for $\beta = 1$ and $D_t^\beta \mathbf{A}_1 \rightarrow \partial \mathbf{A}_1 / \partial t$ [17], where

$$\mathbf{A}_1 = \text{grad}\mathbf{V} + (\text{grad}\mathbf{V})^T \quad (\text{see eq. (1)}).$$

In 1-D form the constitutive equation for second grade liquid is expressed as [19]:

$$\tau(t) = \mu\varepsilon(t) + \alpha_1 D_t^\beta [\varepsilon(t)] \quad (3)$$

$$T_{xx} = T_{yy} = T_{zz} = T_{xz} = T_{yz} = 0, \text{ where } T_{xy} = T_{yx}.$$

II.2. Start-Up Problem

Consider a semi-infinite space filled by a generalized second grade viscoelastic fluid undergoing a transient motion due to tangential shear stress σ exerted on the fluid at $y=0$ (parallel to the x axis). That is, the velocity field is $\mathbf{V} = u(y,t)$, where y is the axis normal to plate surface and u is the velocity component along the x axis.

In this context, the stress tensor component relevant to the present problem is $\mathbf{T}_{xy} = \mu \frac{\partial u}{\partial y} + \alpha_1 D_t^\beta \frac{\partial u}{\partial y}$. In absence of body forces we have: $\rho \frac{D\mathbf{v}}{Dt} = \nabla \cdot \mathbf{T}$ and $\nabla \cdot \mathbf{V} = 0$, that is [17]:

$$\rho \frac{\partial u}{\partial t} = \mu \frac{\partial^2 u}{\partial y^2} + \alpha_1 D_t^\beta \frac{\partial^2 u}{\partial y^2} \quad (4)$$

with initial conditions:

$$u(y,0) = 0, \quad y > 0 \quad (5a)$$

$$t > 0 \quad (5b)$$

$$u \rightarrow 0, \quad y \rightarrow \infty \quad (5c)$$

and a boundary condition:

$$\nu \frac{\partial u(0,t)}{\partial y} + \frac{\alpha_1}{\rho} D_t^\beta \frac{\partial u(0,t)}{\partial y} = -\frac{\sigma}{\rho} \quad (6)$$

$$y = 0; \quad t > 0$$

III. Integral Balance Solution

III.1. Approximate Velocity Profile and Penetration Depth

Following the integral balance methodology [20] the velocity $u(y,t)$ is approximated by a general parabolic profile $u = b_0 + b_1(1 - y/\delta)^n$ with an unspecified exponent n , satisfying the following boundary conditions:

$$u(0,t) = U_s = b_1 \quad (7a)$$

$$u(\delta,t) = 0 \quad (7b)$$

$$\left. \frac{\partial u}{\partial y} \right|_{y=\delta} = 0 \quad (7c)$$

The profile can be expressed as:

$$\frac{u_a}{U_s} = \left(1 - \frac{y}{\delta}\right)^n \quad (8a)$$

or:

$$u_a = U_s \left(1 - \frac{y}{\delta}\right)^n \quad (8b)$$

Here $b_1 = U_s$ is a time-dependent surface velocity defined by the boundary condition (6). The governing equations eq. (5) can be expressed as [6]

$$\frac{\partial u}{\partial t} = \nu \frac{\partial^2 u}{\partial y^2} + p D_t^\beta \frac{\partial^2 u}{\partial y^2} \quad (9)$$

were $p = \alpha_1/\rho [m^2]$ or $p = \nu\lambda_r$ (λ_r is the relaxation time [21]).

Integrating (9) from 0 to δ we get (see detailed explanation of this technique in [22],[23],[24],[25]:

$$\int_0^\delta \frac{\partial u}{\partial t} dy = \int_0^\delta \nu \frac{\partial^2 u}{\partial y^2} dy + \int_0^\delta p D_t^\beta \frac{\partial^2 u}{\partial y^2} dy \quad (10a)$$

$$\int_0^\delta \frac{\partial u}{\partial t} dy = \frac{d}{dt} \int_0^\delta u dy - u|_{y=\delta} \frac{d\delta}{dt} \quad (10b)$$

A substitution of u_a in (6) defines U_s through the equation:

$$\nu \left(-\frac{n}{\delta} U_s\right) + p D_t^\beta \left(-\frac{n}{\delta} U_s\right) = -\frac{\sigma}{\rho} \quad (11)$$

or

$$U_s = \frac{\delta \sigma}{n \mu} \left[1 + \left(\frac{p}{\nu}\right) \frac{1}{(1-\beta)\Gamma(1-\beta)} t^{-\beta} \right]^{-1} \quad (12a)$$

At this point, δ is assumed as a constant, since the problem is about the surface velocity. The equation about δ has to be defined through the integral balance (10a). Further, we denote:

$$U_s = (\delta/n)(B/F) \quad (12b)$$

$$B = \sigma/\mu \quad (12c)$$

$$F = 1 + (p/\nu) j_\beta t^{-\beta} \quad (12d)$$

$$j_\beta = [(1-\beta)\Gamma(1-\beta)]^{-1} \quad (12e)$$

The group $(\delta/n)(\sigma/\mu)$ has a dimension [m/s] (see also eq. (18)). Taking into account the expression for $U_s/\delta = B/nF$ and $U_s\delta = \delta^2(B/nF)$ we get from (10a) (details are available elsewhere [6]) an equation defining δ , namely:

$$\frac{d}{dt} \left(\delta^2 \frac{B}{F} \right) - \nu n(n+1) \frac{B}{F} + n(n+1) p j_\beta \frac{d}{dt} \left(\frac{B}{F} t^{1-\beta} \right) = 0 \quad (13)$$

$$\delta^2 = (\nu t)n(n+1) + n(n+1) p j_\beta t^{1-\beta} + C_1 \quad (14)$$

with $C_1 = 0$, because $\delta(t=0) = 0$, we get:

$$\delta = \sqrt{\nu t} \sqrt{n(n+1)} \sqrt{1 + \frac{p}{\nu} j_\beta t^{-\beta}} \equiv \sqrt{1 + j_\beta D_0} \quad (15)$$

The Deborah number $D_0 = p/\nu t^\beta$ (15) in its general definition is a ratio of two time scales $p/\nu = t_{ev} \Rightarrow t_{ev}/t^\beta = D_0$. Moreover, the process has two characteristic length scales, namely:

- $l_N = \sqrt{\nu t}$ is the length scale in the Newtonian case
- $l_\beta = \sqrt{\nu t^\beta}$ is the fractional length scale (see [6] and [25]).

Therefore, the ratio $p/\nu t^\beta$ is dimensionless and the Deborah number $D_0 = \left(\sqrt{p}/\sqrt{\nu t^\beta} \right)^2$ can be considered as a similarity variable [6]. Further, the approximate velocity profile will be expressed as function of two similarity variables [6]: $\xi = y/\sqrt{\nu t}$ and $\chi = \sqrt{p}/\sqrt{\nu t^\beta}$, ($\chi^2 = D_0$), defined through the characteristic length scales l_N and l_β , respectively.

It is obvious that when $(p/\nu) j_\beta t^{-\beta}$ becomes negligible ($j_\beta D_0 \approx 10^{-3}$ could be assumed as negligible), the flow becomes Newtonian and the penetration depth reduces to $\delta = \sqrt{\nu t} \sqrt{2n(n+1)}$ [6], [26], [27].

III.2. Dimensionless Velocity Profile

Therefore, with the expression (15) of δ the velocity profile is:

$$\frac{u}{U_s} = \left(1 - \xi \frac{1}{F_n \sqrt{1 + j_\beta \chi^2}} \right)^n = \left(1 - \frac{\xi}{F_n R_\beta} \right)^n \quad (16)$$

where $\xi = y/\sqrt{\nu t}$ is the Boltzmann similarity variable, and:

$$F_n = \sqrt{n(n+1)}, \quad R_\beta = \sqrt{1 + j_\beta D_0}, \quad (R_\beta = \sqrt{1 + j_\beta \chi^2}) \quad (17)$$

Further, with $\delta = \sqrt{\nu t} F_n R_\beta$ and $B = \sigma/\mu$, the surface velocity can be expressed as:

$$U_s = \left(\frac{\sigma \sqrt{\nu t}}{\mu} \right) \left(\frac{F_n}{n R_\beta} \right) \quad (18)$$

Then the approximate profile becomes:

$$u = U_s \left(1 - \frac{\xi}{F_n R_\beta} \right)^n \quad (19)$$

In the Newtonian problem the exact solution is $u/U_s = 1 - \text{erf}(\xi/2)$ with $0 \leq \xi \leq \infty$. However, in the integral-balance solution of the Newtonian problem, we have $0 \leq \xi \leq F_n$, while for the viscoelastic flow the range is $0 \leq \xi \leq F_n R_\beta$. Moreover, from the terms of (12a), (12b) we have $U_s = (\delta/n)(B/F)$. Then with $F = 1 + p j_\beta t^{-\beta}$ we get $F = (1 + D_0 j_\beta) = \nu (R_\beta)^2$ (see eq. (12a)).

The group $\sigma \sqrt{\nu t}/\mu$ in (18) has a dimension of velocity [m/s]. The problem solved here, to some extent, is an analogue of the Newman problem in the diffusion (heat or mass) where under imposed constant surface flux, the surface temperature increases in time. Moreover, the problem has no characteristic time and length scales. The term $\sqrt{\nu t}$ [m] is like a length scale, as in any other semi-infinite diffusion problems, while σ/μ [s] can be used as a time scale.

III.3. Approximate vs. Exact Solution: a Preliminary Analysis

The exact solution of the problem has been developed by Hayat et al. [17] and can be expressed as (A-2) (see the Appendix):

$$u(y,t) = \left(\frac{\sigma\sqrt{vt}}{\mu}\right)\Phi_1(\beta,t,p,\nu) + \left(\frac{\sigma\sqrt{vt}}{\mu}\right)\Phi_2(y,\beta,t,p,\nu) \quad (20a)$$

The terms Φ_1 and Φ_2 are commented in the Appendix. In general Φ_1 represents the time variations of the surface velocity U_s , while the flow field in the fluid depth is depicted by Φ_2 . Moreover, in the Appendix some terms are re-arranged in order to express the exact solution through the similarity variables $\xi = y/\sqrt{vt}$ and $\chi = \sqrt{p}/\sqrt{vt}^\beta$, because it is hard the original version [17] to be used for a physical analysis. In contrast, the integral balance solution yields an entire domain approximate profile allowing the physical effects to be represented by separate terms through ξ and χ , and the fractional-order correction factor j_β . As to the errors in solutions, the exact solution also can be considered as an approximate one when the infinite sums in Φ_1 and Φ_2 are truncated in practical calculations.

The common term $(\sigma\sqrt{vt}/\mu)$ in both the exact and the approximate solutions only confirms the physical adequacy of the approach developed here, while the time-dependent and the flow-field terms differ and are strongly affected by the approach to solve the problem. At the free surface ($y = 0$), for instance, we have:

$$u(0,t) = (\sigma\sqrt{vt}/\mu)\Phi_1(\beta,t,p,\nu) \quad (20b)$$

and:

$$u_a(0,t) = U_s = (\sigma\sqrt{vt}/\mu)(F_n/nR_\beta) \quad (20c)$$

The numerical experiments reported further in this article will illustrate the differences in both solutions.

III.4. Calibration of the Exponent

First we can consider the limiting case with $D_0 = 0$, which has been analyzed thoroughly in its heat-diffusion version [22],[23],[28]. With calibration at $y = 0$ [26], we have $n = 1.675$, while the minimization of the L_2 norm in the domain $0 \leq y \leq \delta$ results in $n \approx 2.35$ [28] and $n \approx 1.507$ applying a similarity transform of eq. (93) at $p = 0$ [29].

The general approach in estimation of the optimal exponent is to minimize the L_2 norm in the domain $0 \leq y \leq \delta$, [6],[22],[25], namely:

$$E(y,t,\beta) = \int_0^\delta \left[\frac{\partial u}{\partial t} - \nu \frac{\partial^2 u}{\partial y^2} - pD_t^\beta \frac{\partial^2 u}{\partial y^2} \right]^2 dy \rightarrow \min \quad (21)$$

After integration in (21) we get $E(y,t,\beta) = \frac{e_n(y,t,\beta)}{(vt)^{3/2}} \equiv \frac{e_n(y,t,\beta)}{\delta^3}$.

Taking into account that the entire function $E(y,t,\beta)$ decays in time with a speed $\equiv \delta^3$, the minimization refers to an optimal value of n minimizing the function $e_n(y,t,\beta)$. Setting all time-dependent terms (increasing in time only) of $e_n(y,t,\beta)$ equal to zero (see [22],[24],[25] and [28]), we get:

$$e_n(y,\beta,t=0) = \nu^2 \frac{(n-1)}{2} - \frac{\nu p}{t^\beta} n^2 (n-1) \quad (22a)$$

$$n \approx \frac{1}{\sqrt{2}} \frac{1}{\sqrt{D_0}} \quad (22b)$$

The result is just the same as that developed in [6].

Numerical experiments [6] with $n = 2$ and $n = 3$ provide $D_0 \approx 0.125$ and $D_0 \approx 0.055$, respectively. In this context, the optimal Newtonian profile with exponents we get: $n \approx 2.35$ corresponds to $D_0 \approx 0.100$, while that $n \approx 1.507$ provides $D_0 \approx 0.220$. Therefore, within the range defined by $O(D_0) \sim 1$, that is the viscoelastic flow [21], the exponent of the parabolic profile oscillates around $n = 2$ as the value of D_0 varies. Taking into account, the inverse time dependence of D_0 , it is reasonably to expect and increase in the value of the exponent $n \sim t^{\beta/2}$ (see (22b)). That is, the shorter relaxation times (the larger observation times), the larger exponents of the approximate profile and *vice versa*. For $n = 2$, for instance, we get:

$$\frac{u}{U_s} \approx \left(1 - \frac{y}{3.464\sqrt{vt}\sqrt{1+j_\beta D_0}} \right)^2 \quad (23a)$$

$$\frac{u}{U_s} \approx \left(1 - \frac{\xi}{3.464\sqrt{1+j_\beta \chi^2}} \right)^2 \quad (23b)$$

IV. Numerical Experiments and Analyses

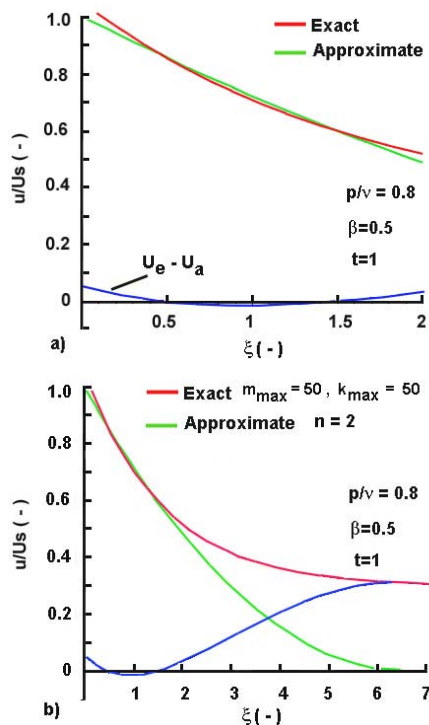
IV.1. Approximate vs. Exact Solution

A) Fixed exponent

Some numerical experiment was performed to compare the developed approximated solution with the

exact one [17] in case of affixed value of $n = 2$. In fact, the exact solution [17] never have been plotted, or at least tested numerically, so far. The sums in (A-1) were truncated to $m_{max} = 50$ and $k_{max} = 50$. Then, the solutions were performed by Maple 13. In general, both the approximate and the exact solution almost match for $0 \leq \xi \leq 2$ (see Figs. 1(a), (b)) and p/ν ratios close to 1. The plots are for $\beta = 0.5$ as a frequently used fractional order in numerical experiments.

The tests with the exact solution with $0.1 \leq \beta \leq 0.5$, in fact below $\beta \approx 0.4$, are disappointing because the exact solution becomes unstable. These results (not shown here) focus on a new problem beyond the scope of the present work.



Figs. 1. Numerical tests with the exact solution and the approximate one with a fixed exponent

Besides, with increase in the range of variations of ξ beyond $\xi \approx 1.5$, precisely with $2 \leq \xi \leq 7$ the difference between the exact and the approximate solutions becomes enormous. Even with $m_{max} = 100$ and $k_{max} = 100$ does not approach zero. This an inherent problem of the integral balance solution for the classical diffusion equations ($p = 0$) when a fixed exponents for the entire domain is used [TS-2010], i.e. with the increase in ξ the approximate solution goes faster to zero than the exact one. This can be fixed, to some extent, by a self-adaptive exponent varying with increase in ξ . This problem will be commented further in this work.

At this moment, we refer to impossibility to express the exact solution completely by the similarity variables ξ and χ because the time-dependent sums in both Φ_1 and Φ_2 (see A-5 and A-6) cannot be converted easily into dimensionless groups. Hence, there are inherent problems, coming from the approaches used to develop the solutions at issue, hindering the direct comparison of the final results.

In the calculations demonstrated by the plots, the time was chosen $t = 1$. This means that the variations in ξ are due to variations in the space co-ordinate y , at given physical proprieties of the fluid, of course. Therefore, for $\xi < 1.5$, i.e. at short distances from the surface, where the shear is exerted, the approximate solution with a fixed exponent provides adequate and acceptable results.

B) Variable exponent: some approximations

The variable exponent approach has been tested successfully to classical parabolic equations [29]. Some attempts based on empirical relationships $n = n(\xi)$ and to fractional-time subdiffusion equations ere reported in [24]. The main idea comes from the estimates (22b) and the fact that $n \sim t^\beta$ (see the earlier comments about eqs. 22). From this point of view, with a fixed value of p/ν , as fractional time scale and with variations in time (i.e. variations in ξ) we get from (22b):

- Large times

$$t \uparrow \sim \xi \downarrow \Rightarrow (p/\nu)t^{-\beta} \downarrow \Rightarrow (1/(p/\nu)t^{-\beta}) \uparrow \Rightarrow n \uparrow \quad (24a)$$

- Short times

$$t \downarrow \sim \xi \uparrow \Rightarrow (p/\nu)t^{-\beta} \uparrow \Rightarrow (1/(p/\nu)t^{-\beta}) \downarrow \Rightarrow n \downarrow \quad (24b)$$

Here, the symbols \uparrow and \downarrow mean that the value increase or decrease.

Therefore, with large a time, which is with small ξ for a fixed y , the exponent should decrease in time, and *vice versa*. However, this estimate is based only on the analysis of the fractional correction R_β . When at large time $R_\beta \rightarrow 1$ the Newtonian behaviour dominates, the estimate established in [29] teaches that n should increase as ξ increases, behaviour just opposite to that established above. From this point of view, the choice of adequate exponent should be separated in two, namely:

- a) short-time solutions with dominating visco-elastic effects and approximate profiles and exponent n controlled by a relationship based on the estimates (24a),(24b).

b) Large time solutions, with a Newtonian behaviour, where n increases with the increase in ξ and can be modeled as $n(\xi) = n_0 + k_j \text{LambertW}(\xi)$ [29], where $k_j \approx 0.5$ and $\text{LambertW}(\xi)$ is the Lambert function.

In this context, the variable exponent can be suggested as:

$$n(\zeta, \chi) = \frac{n(\zeta)}{\sqrt{1+k_b D_0}} = \frac{[n_0 + k_j \text{LambertW}(\xi)]}{\sqrt{1+k_b \left(\frac{p}{v}\right) \frac{1}{t^\beta}}} \quad (25)$$

The value of n_0 come from the calibration of the Newtonian profile at $y=0$ [29] and for the problem solved here it is $n_0 \approx 3.65$.

The numerical tests reveal some features of both the approximate and the exact solutions, among them:

- a) The best results were developed for $(p/v) \sim O(1)$ and $0.5 \leq \beta < 1$. The weighting coefficients $k_b = 0.5$ and $k_j = 0.5$ are the best chosen for the numerical calculations. Plots are shown in Fig. 2.
- b) The exact solution is quite sensitive with respect to the number of terms in the time-dependent sums; Worst results were obtained $m_{max} = 5$ and $k_{max} = 5$. Increase in the number of the terms beyond $m_{max} = 50$ and $k_{max} = 50$ and best results does not affect the solution. Numerical examples are shown in Figs. 3 (see also Fig. 1(b) and Fig. 2)
- c) The exact solution is very sensitive with respect to the value of the fractional order $\beta < 0.5$. The best and physically adequate results were obtained for $0.5 \leq \beta < 1$. The approximate solution does not show instabilities. The illustrations of these effects are shown in Fig. 4.
- d) The exact solution is very sensitive with respect to the ratio p/v . Large variations in p/v (beyond 1.25 and below 0.8) result in instable behaviour of the exact solution while the approximate one is insensitive. Illustrative plots are shown in Fig. 5.

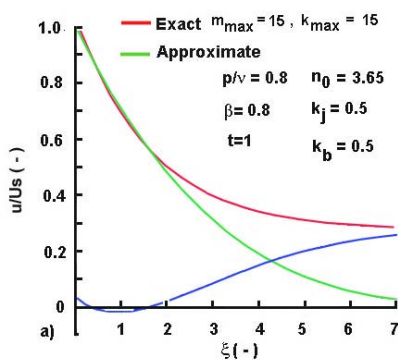
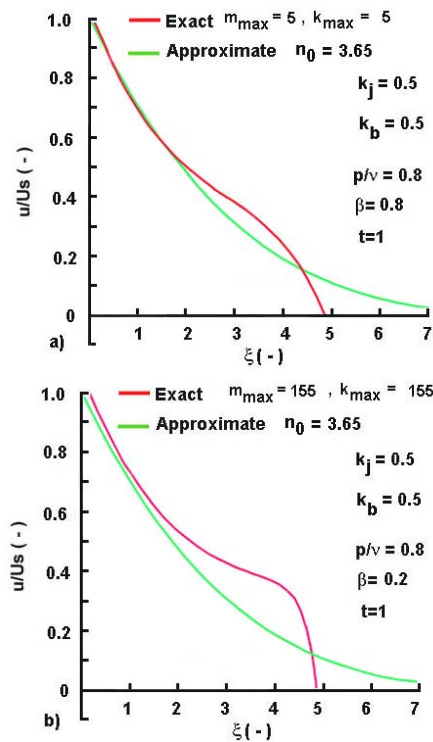


Fig. 2. The best matching solutions for $(p/v) \sim O(1)$ and $0.5 \leq \beta < 1$



Figs. 3 Effect of the number of the terms in the sums of the exact solution, i.e. effects of the truncations on the solutions. Additionally on Fig. 3(b), it is seen the effect of fractional order β . See also Fig. 4

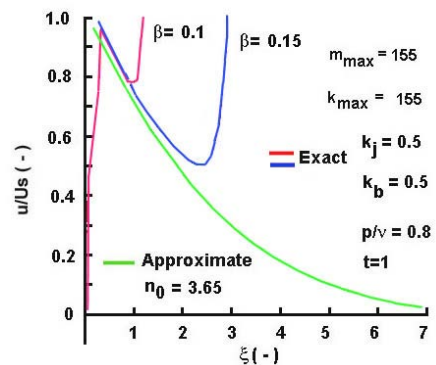


Fig. 4. Effect of fractional order $\beta < 0.5$ on the exact solutions. The calculation conditions are the same as those used for $\beta \geq 0.5$

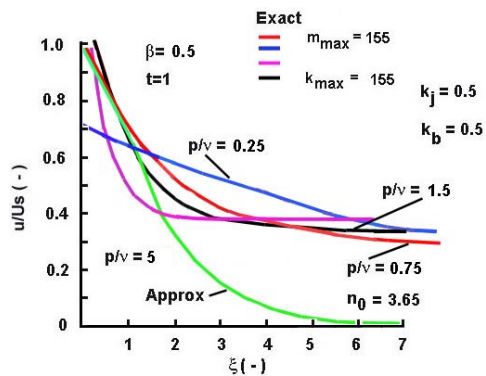


Fig. 5. Effect of the magnitude of the ratio p/v on the behavior of the exact solution

V. Conclusion

This is an attempt to apply a classical integral method which is a moment method from weighted-residuals' family with a weighting function equal to 1.

The approximate solution has well disguised terms repressing the effects of both the Newtonian viscosity and the visco-elasticity. The solution clearly indentifies two similarity variables controlling fluid flow and corresponding separately to these effects.

The entire domain approximation is simple but with some restrictions imposed by the fixed exponent of the parabolic profile and the short range (with respect to ξ) approximation.

The minimization of L_2 avoids some of these drawbacks and yields an explicit result that the exponent is time-dependent. This confirms the relationship developed in [29] where similar problem with $p = 0$ is developed. Moreover, combining the results from [29] and the present estimate (22b), the concept of a variable (self-adaptive) exponent (25) was conceived.

The developed approximate solution was compared to the exact one [17], but many questions rose mainly concerning the numerical simulations of the exact solution.

Appendix

The exact solution developed by Hayat et al. [17] (represented by the variables used in the present work):

$$u(y,t) = \frac{\sigma}{\mu\sqrt{p\nu}} \sum_{m=0}^{\infty} \frac{\Gamma(1/2+m) [-(\alpha_1/\nu)^{-1}]^m t^{-1+m\beta+(3+\beta)/2}}{m! \Gamma(1/2) \Gamma[m\beta+(3+\beta)/2]} + \frac{\sigma}{\mu\sqrt{p\nu}} \times \sum_{k=1}^{\infty} \frac{[-y/p^{1/2}]^k}{k!} \sum_{m=0}^{\infty} \frac{\Gamma[(k+1)/2+m] [-(p/\nu)^{-1}]^m t^{-1-k/2+m\beta+k\beta/2+(3+\beta)/2}}{m! \Gamma[(k+1)/2] \Gamma[(k+1)/2] \Gamma[-k/2+m\beta+k\beta+(3+\beta)/2]} \quad (\text{A-1})$$

From the point of view of the approximate solution developed (A-1) can be presented as:

$$u(y,t) = \left(\frac{\sigma\sqrt{vt}}{\mu} \right) \Phi_1(\beta,t,p,\nu) + \left(\frac{\sigma\sqrt{vt}}{\mu} \right) \Phi_2(y,\beta,t,p,\nu) \quad (\text{A-2})$$

$$\Phi_1(\beta,t,p,\nu) = \frac{1}{\sqrt{pt}} \sum_{m=0}^{\infty} \frac{\Gamma(1/2+m) [-(p/\nu)^{-1}]^m t^{-1+m\beta+(3+\beta)/2}}{m! \Gamma(1/2) \Gamma[m\beta+(3+\beta)/2]} \quad (\text{A-3})$$

$$\Phi_2(y,\beta,t,p,\nu) = \frac{1}{\sqrt{pt}} \sum_{k=1}^{\infty} \frac{(-y/\sqrt{vt})^k (vt/p)^{k/2}}{k!} \sum_{m=0}^{\infty} \frac{\Gamma[(k+1)/2+m] [-(p/\nu)^{-1}]^m t^{-1-k/2+m\beta+k\beta/2+(3+\beta)/2}}{m! \Gamma[(k+1)/2] \Gamma[(k+1)/2] \Gamma[-k/2+m\beta+k\beta+(3+\beta)/2]} \quad (\text{A-4})$$

The term Φ_1 represents only the variations in the surface velocity U_s in time. The second term Φ_2 describes the flow field in depth of the liquid. In this context, for $y = 0 \rightarrow \Phi_2 = 0$. Furthermore, in Φ_2 we have $\xi = y/\sqrt{vt}$ and $(vt/p) \rightarrow 1/\chi^2 = 1/D_0 = vt^\beta/p$ for $\beta = 1$. Moreover:

$$\left(\frac{1}{\sqrt{pt}} \right) \times \sum_m^{\infty} [-(p/\nu)^{-1}]^m t^{-1+m\beta+(3+\beta)/2} \text{ in } \Phi_1 \quad (\text{A-5})$$

and:

$$\left(\frac{1}{\sqrt{pt}}\right) \times \sum_{k=1}^{\infty} \frac{(vt/p)^{k/2}}{k!} \sum_{m=0}^{\infty} \left[-(p/v)^{-1}\right]^m t^{-1-k/2+m\beta+k\beta/2+(3+\beta)/2} \text{ in } \Phi_2 \quad (\text{A-6})$$

correspond to decaying elastic effects (the fractional order term in the governing equation) represented in the approximate solution by the term $R_\beta = \sqrt{1 + j_\beta D_0}$ (see eq.(18) and eq.(19)).

Acknowledgements

The work was supported by the grant N10852/2011 of Univ. Chemical Technology and Metallurgy (UCTM), Sofia, Bulgaria.

References

- [1] Naraim, A., Joseph, D.D., Remarks about the interpretations of impulsive experiments in shear flows of viscoplastic liquids, *Rheologica Acta*, 22 (1983) 528-538.
- [2] Aiboud, S., Saouli, S., Thermodynamic Analysis of Viscoelastic Magnetohydrodynamic Flow over a Stretching Surface with Heat and Mass Transfer, *Int. Rev. Chem. Eng.* 3 (2009) 315-324.
- [3] Tan, W., Xu, M., The impulsive motion of a flat plate in a generalized second grade fluid, *Mech. Res. Com.* 29 (2002) 3-9.
- [4] Tan, W., Xu, M., Plane surface suddenly set in motion in a viscoelastic fluid with fractional Maxwell model, *Acta Mech. Sin.*, 18 (2002) 342-349.
- [5] Jordan, P.M., A note on start-up, plane Couette flow involving second-grade fluids, *Mathematical Problems in Engineering*, 2005 (2005) 539-545.
- [6] Hristov, J. Integral-Balance Solution to the Stokes' First Problem of a Viscoelastic Generalized Second Grade Fluid, *Thermal Science*, 16 (2012),2, (In press). DOI:10.2298/TSCI110401077H
- [7] Bandelli, R., Rajagopal, K. R., Start-up flows of second grade fluids in domains with one finite dimension, *Int. J. Non-Linear Mechanics*, 30 (1995) 817-839.
- [8] Derkach, S.R., Rheology on the Way from Dilute to Concentrated Emulsions, *Int. Rev. Chem. Eng.* 2 (2009) 465-472.
- [9] Siginer, D.A., Letelier, M.F., Laminar flow of non-linear viscoelastic fluids in straight tubes of arbitrary contour, *Int J Heat Mass Trans.* 54 (2011) 2188-2202.
- [10] Hsiao, K.L., Manufacturing Extrusion Process for Forced Convection Micropolar Fluids Flow with Magnetic Effect over a Stretching Sheet, *Int. Rev. Chem. Eng.* 1 (2009) 272-276.
- [11] Hsiao, K.L., Manufacturing Extrusion Process for Magnetic Mixed Convection of an Incompressible Viscoelastic Fluid over a Stretching Sheet, *Int. Rev. Chem. Eng.* 1 (2009) 164-169.
- [12] Karimi S., Dabir, B., Dadvar, M., Non-Newtonian Effect of Blood in Physiologically Realistic Pulsatile Flow, *Int. Rev. Chem. Eng.* 2 (2009) 805-810.
- [13] Schmitt, C., Henni, A.H., Cloutier, G., Characterization of blood clot viscoelasticity by dynamic ultrasound elastography and modeling of the rheological behavior, *J. Biomech.*, 44 (2011) 622-629.
- [14] Pfitzenreiter, T., A physical basis for fractional derivatives in constitutive equations, *ZAMM*, 84 (2004) 284-287. doi 10.1002/zamm.200310112.
- [15] Kang, J., Xu, M., Exact solutions for unsteady unidirectional flows of a generalized second-order fluid through a rectangular conduit, *Acta Mech. Sin.*, 25 (2009) 181-186. doi 10.1007/s10409-008-0209-3.
- [16] Qi, H., Xu, M., Some unsteady unidirectional flows of a generalized Oldroyd-B fluid with fractional derivative, *Appl. Math. Model.* 33 (2009) 4184-4191.
- [17] Hayat, T., Asghar, S., Siddiqui, A.M., Some unsteady unidirectional flows of a non-Newtonian fluid, *Int. J. Eng. Sci.* 38 (2000) 337-346.
- [18] Tan, W., Xu, M., Unsteady flows of a generalized second grade fluid with the fractional derivative model between two parallel plates, *Acta Mech. Sin.*, 20 (2004) 471-476.
- [19] Tan W., Xian F., Wei L., An exact solution of unsteady Couette flow of generalized second grade fluid, *Chinese Science Bulletin*, 47 (2002) 1783-1785.
- [20] Goodman T.R., Application of Integral Methods to Transient Nonlinear Heat Transfer, *Advances in Heat Transfer*, T. F. Irvine and J. P. Hartnett, eds., 1 (1964), Academic Press, San Diego, CA, pp. 51-122.
- [21] Goodwin, J.W., Hughes, R.W., Rheology for chemists: An Introduction, 2nd ed, RSC Publishing, Cambridge, UK., 2008.
- [22] Hristov J., Heat-Balance Integral to Fractional (Half-Time) Heat Diffusion Sub-Model, *Thermal Science*, 14 (2010) 291-316. doi: 10.2298/TSCI1002291H.
- [23] Hristov J., A Short-Distance Integral-Balance Solution to a Strong Subdiffusion Equation: A Weak Power-Law Profile, *Int. Rev. Chem. Eng.*, 2 (2010) 555-563.
- [24] Hristov J., Approximate Solutions to Fractional Subdiffusion Equations: The heat-balance integral method, *The European Physical Journal-Special Topics*, 193(2011) 229-243. DOI:10.1140/epjst/e2011-01394-2
- [25] Hristov J., Starting radial subdiffusion from a central point through a diverging medium (a sphere): Heat-balance Integral Method, *Thermal Science*, 15 (2011), S5-S20. doi: 10.2298/TSCI1101S5H
- [26] Hristov, J., The heat-balance integral method by a parabolic profile with unspecified exponent: Analysis and benchmark exercises, *Thermal Science*, 13 (2009) 22-48.
- [27] Hristov, J., Research note on a parabolic heat-balance integral method with unspecified exponent: an entropy generation approach in optimal profile determination, *Thermal Science*, (2) (2009) 27-48, doi:10.2298/TSCI0902049H.
- [28] Myers, T.G., Optimal exponent heat balance and refined integral methods applied to Stefan problem, *Int. J. Heat Mass Transfer*, 53 (2010), 5-6, pp. 1119-1127.
- [29] Hristov, J. The Heat-Balance Integral: 2.A Parabolic profile with a variable exponent: the concept and numerical experiments, *CR Mechanique* (in Press).

Authors' information



Jordan Hristov is associate professor of Chemical Engineering at the University of Chemical Technology and Metallurgy, Sofia, Bulgaria. Relevant information is available at <http://hristov.com/jordan>.
E-mail: jordan.hristov@mail.bg